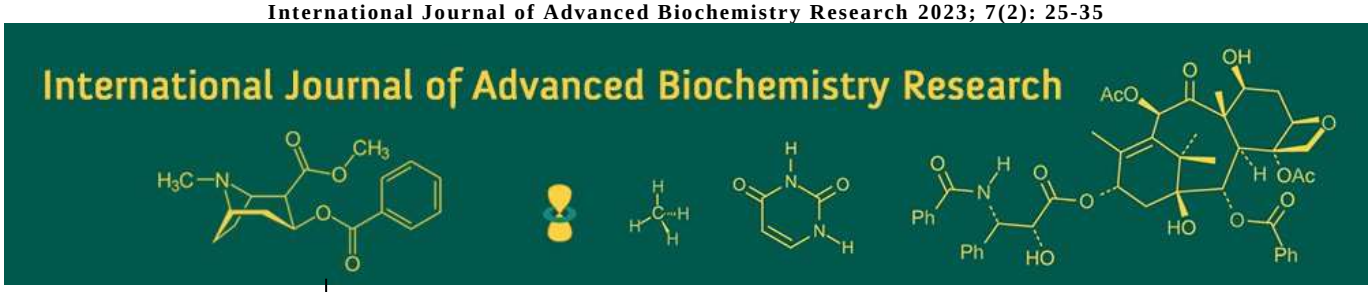

ISSN Print: 2617-4693
ISSN Online: 2617-4707
IJABR 2023; 7(2): 25-35
www.biochemjournal.com
Received: 10-06-2023
Accepted: 12-07-2023

Nitya P Doshi
A) M.P. Mills Compound Road, Balkrishna Nakashe Marg, Janata Nagar, Tardeo, Mumbai, Maharashtra, India
B) Department Of Chemistry, Vidyanagari, University of Mumbai, Santacruz (E). Mumbai, Maharashtra, India

Sanket S Shirodkar
Bombay College of Pharmacy, Kolivery Village, Mathuradas Colony, Kalina, Vakola, Santacruz East, Mumbai, Maharashtra, India

Corresponding Author:
Yakubu OE
Department of Biochemistry, Federal University, Wukari, Taraba State, Nigeria

One-Pot synthesis of biologically active bimetallic Ag-Zn Nanoparticles using Madagascar periwinkle (Sadaafuli) plant extract

Nitya P Doshi and Sanket S Shirodkar

DOI: https://doi.org/10.33545/26174693.2023.v7.i2a.212

Abstract
Nanoparticles (NPs) have been widely studied in various fields due to their unique properties and potential applications. Among the various types of nanoparticles, bimetallic nanoparticles have gained significant attention due to their enhanced catalytic activity and stability compared to monometallic nanoparticles. Various physical and chemical methods have been developed for the synthesis of bimetallic nanoparticles. However, these methods have several limitations such as the use of toxic reducing agents, high energy consumption, and the need for multiple steps. Therefore, developing a simple, eco-friendly, and cost-effective approach for the synthesis of bimetallic nanoparticles is highly desirable. Plants contain a variety of chemicals that work not only as potential treatments for cancer, among other illnesses, but also as powerful reducing and stabilising agents in the synthesis of nanoparticles. This paper discusses the use of *Catharanthus roseus* (Madagascar periwinkle) leaf extract in the synthesis of non-toxic, environmentally-friendly and inexpensive bimetallic silver-zinc NPs. The synthesized NPs were characterized using techniques like infrared (IR) spectroscopy, UV-visible spectroscopy (UV-Vis), dynamic light scattering (DLS), scanning electron microscopy (SEM). The NPs were discovered to be 8 nm in size with a zeta potential of -38 mV, illustrating their stability. UV-Vis confirmed the presence of Ag-Zn NPs in an alloy structure with absorption peaks at 416 and 380 nm. These Ag-Zn NPs were tested for antimicrobial and anticancer activity. The synthesized nanoparticles showed promising anticancer and antimicrobial activity, which may have potential applications in various fields, such as biomedical, biosensors, and nanomedicine.

Keywords: Bimetallic nanoparticles, green synthesis, anticancer activity, antimicrobial activity, Madagascar Periwinkle

1. Introduction
Progress in nanotechnology has had benefits in the biomedical world, ranging from diagnosis of ailments to treatment for fatal disorders such as cancer. Due to its unique physiochemical, electrical, catalytic and optical features, [1-3] and therefore plethora of applications, nanotechnology has attracted the attention of researchers [4] in fields such as sewage treatment, food, optoelectronics and cosmetics [5-8]. Bimetallic nanoparticles (NPs) have notably caught the interest of research in recent years due to their significant differences in their properties [9]. For instance, they have different structures and morphologies due to their composition of two different metal elements [10].
Different methods of NP synthesis include chemical and biological/green synthesis. In chemical methods, various chemical precursors are used to synthesize NPs, which can have detrimental effects on the environment due to their toxicity [11]. Moreover, these chemicals limit the colloidal agglomeration and restrict the application of NPs in clinical and biomedical fields [12]. A less expensive method of NP synthesis is the green method, which uses environmentally friendly reducing agents – such as plant extracts – to aid NP synthesis. [13, 14] This method is also eco-friendly, simple, rapid, and renewable [15].
In the green synthesis of bimetallic NPs, two aqueous metal precursor solutions are mixed with a plant extract. The plant's phytochemicals present in the extract are believed to act as reducing and stabilizing agents, effectively reducing metal ions into metal NPs. In theory, metal ions with a stronger reduction potential are reduced faster than metal ions with a weaker reduction potential, thereby forming a core-shell structure with the faster-reduced ions being the nucleus [1, 16].

C. roseus, an evergreen plant with origins in Madagascar, is widely used in traditional Ayurvedic medicine due to its antitumor, antimicrobial and antioxidant effects. It contains various phytochemicals such as alkaloids, flavonoids, and terpenoids, which have been reported to have various biological activities. It is known to contain vincristine and vinblastine, which are used as treatments for various types of cancers such as breast cancer, and lymphoblastic leukemia. [17-23]. The plant shows potential for the synthesis of silver NPs but requires investigation in the synthesis of bimetallic NPs [24-28].

Therefore, in this study, we present a one-pot synthesis of biologically active bimetallic Ag-Zn nanoparticles using Madagascar periwinkle as a reducing and capping agent to explore the possibility of a safe and environmentally-friendly anticancer treatment option. The synthesized Ag-Zn nanoparticles showed promising biological activity, which may have potential applications in various fields. A simple schematic representation of the method is depicted in Figure 1.

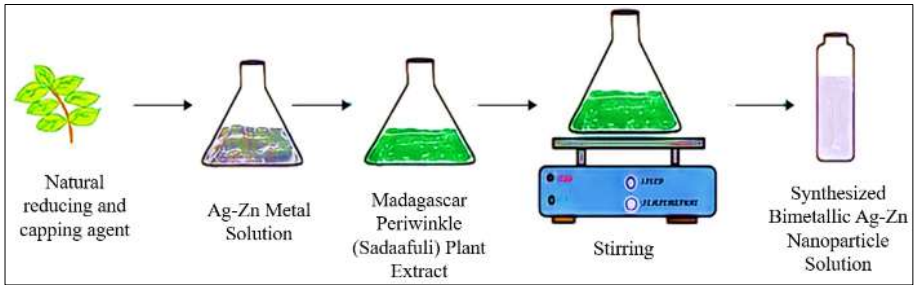

Fig 1: Schematic representation of one-pot synthesis method of bimetallic nanoparticles

2. Material and Method

In this study, Madagascar periwinkle leaves were gathered from Solapur and meticulously cleaned. After drying at 60°C and grinding into powder. Bimetallic Ag-Zn nanoparticles were synthesized using high-quality silver nitrate and zinc sulfate obtained from Sigma Aldrich, INDIA. The entire process involved the use of double distilled water as a solvent.

2.1 Preparation of Madagascar Periwinkle Extract

The methodology for extracting a plant extract from Madagascar periwinkle leaves involved the following steps:

Leaf Grinding: The desiccated Madagascar periwinkle leaves were meticulously pulverized into a finely powdered state using a mortar and pestle.

Suspension Preparation: Approximately 7.5 grams of the powdered leaves were amalgamated with 100 ml of deionized water inside a round-bottom flask.

Reflux Process: The resulting mixture was subjected to a reflux process, maintained at a temperature of 60°C for a duration of 2 hours, with continuous agitation.

Filtration and Filtrate Collection: Subsequent to the reflux, the mixture was subjected to filtration using Whatman filter paper, facilitating the accumulation of the filtrate in a designated beaker.

Concentration via Rotary Evaporation: The obtained filtrate underwent concentration using a rotary evaporator, operating under conditions of reduced pressure and at a temperature of 40°C.

Formation of Concentrated Extract: The outcome of the concentration process resulted in a concentrated extract, which was subsequently harnessed as a reducing agent for the synthesis of Ag-Zn nanoparticles.

This synthesized extract was subjected to characterization through UV-Vis spectroscopy, verifying the existence of phytochemical constituents within the extract.

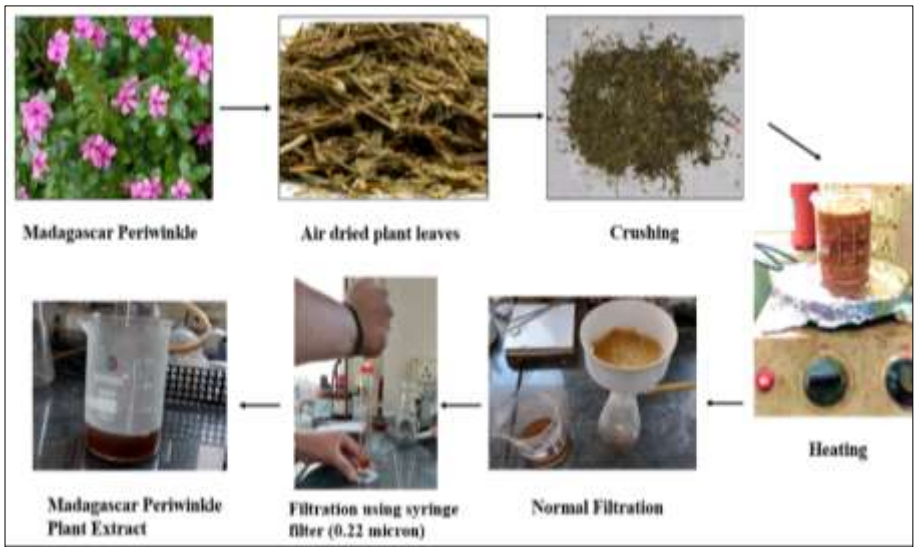

Fig 2: Plant extract preparation method

2.2 Preparation of Bimetallic Ag-Zn NPs

The procedure for creating bimetallic Ag-Zn nanoparticles using Madagascar periwinkle extract as a reducing agent encompassed these steps:

Preparation of Metal Solutions: Solutions of 12 mM silver nitrate and 6 mM zinc sulfate were separately crafted using deionized water.

Mixture Formation: Within a round-bottom flask, 10 ml of each solution were combined and subjected to magnetic stirring at room temperature.

Addition of Extract: Gradually, 6 ml of Madagascar periwinkle extract were introduced dropwise into the mixture. The reaction was sustained for 24 hours at room temperature under constant stirring.

Color Change as Reaction Indicator: Over time, the mixture's color transitioned from colorless to a deep brown, indicating the successful formation of Ag-Zn nanoparticles.

Centrifugation for Purity: To eliminate unreacted materials and residual plant extract, the resulting nanoparticles were purified through centrifugation at 10,000 rpm for 10 minutes.

This systematic process yielded bimetallic Ag-Zn nanoparticles, evident from the color shift and the subsequent purification procedure.

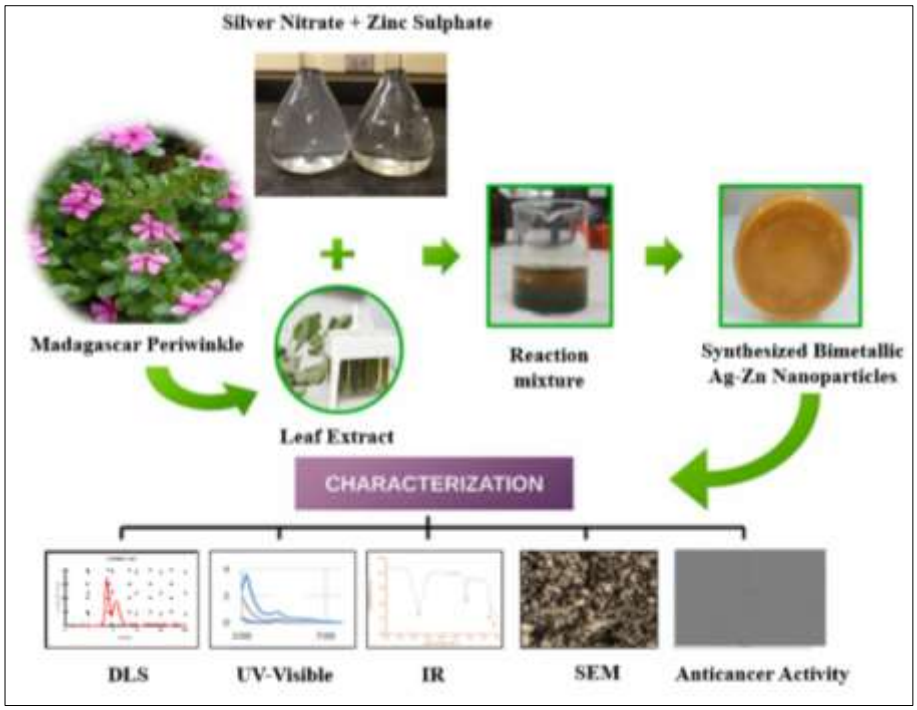

Fig 3: Preparation method of Ag-Zn bimetallic nanoparticles

2.2 Evaluation of Anticancer activity by MTT assay

Requirements:

1. MTT Powder (the solution is filtered through a 0.2 µm filter and stored at 2-8 °C for frequent use or frozen for extended periods)
2. DMSO
3. Trypan blue
4. Phosphate Buffered Saline (PBS)
5. Trypsin
6. CO_2 incubator
7. Centrifuge
8. Hemocytometer

Assay protocol

Cell Preparation: Cervical Cancer cells

HeLa cells (Grown in DMEM media supplemented with 10% Fetal Bovine Serum), harvested using trypsin, and counted using Trypan blue and a hemocytometer.

- Collected the cells when they reach about 70-80% confluence
- Checked for the viability and centrifuged the cells

Procedure: Day 1, seed 2,500-5,000 cells/well (HeLa) in their exponential growth phase in 100 µL volume in a flat-bottomed 96-well polystyrene coated plate (Thermo Scientific Nunc 96-well plate, Nunclon Delta-white color with lid). Incubate overnight at 37 °C with 5% CO_2 to allow cell adhesion.

1) Day 2, after 24 hours of seeding, the concentration of nanodrugs (test compounds) were diluted in cell culture medium at different concentration (5, 25, 65 and 100 µg/ml) in DMEM without FBS containing a final volume of 100 µl/well. Incubated for 24 hour. Experiments done in triplicate.
2) Day 3, after 24 hour of incubation, added 10 µL of MTT solution (5 mg/10 ml of MTT in 1X PBS) into each well. Wrapped the plate in aluminium foil and incubated for 3-4 hours at 37 °C, 5% CO_2 incubator, protected from light.
   Note: Depending on the individual cell type and concentration used, longer incubation times may be necessary.
3) Formazan crystals formed after 3-4 hours in each well were dissolved in 100 µl DMSO solution (solubilizing buffer).
4) Read absorbance at 590 nm. Read plate within 1 hour [32-34].

5) The positive control wells contain untreated cells, MTT solution and a solubilizing buffer.
6) The blank in the MTT assay is a cell-free medium plus an MTT solution and a solubilizing buffer.
7) Experiments were repeated three times for the average calculations.

Viability is defined as a percentage of live cells in a whole population or in other words, cell viability is defined as the number of healthy cells in a solution.

% Viability = Sample/Control x100

Sample: Mean value of the measured optical density (OD)/Absorbance of the Nanodrugs

Control: Mean value of the measured optical density (OD)/Absorbance of the Control

Result and Discussion

Dynamic Light Scattering (DLS)

The size of nanoparticles is measured using DLS, and their stability in suspension over time is also assessed.

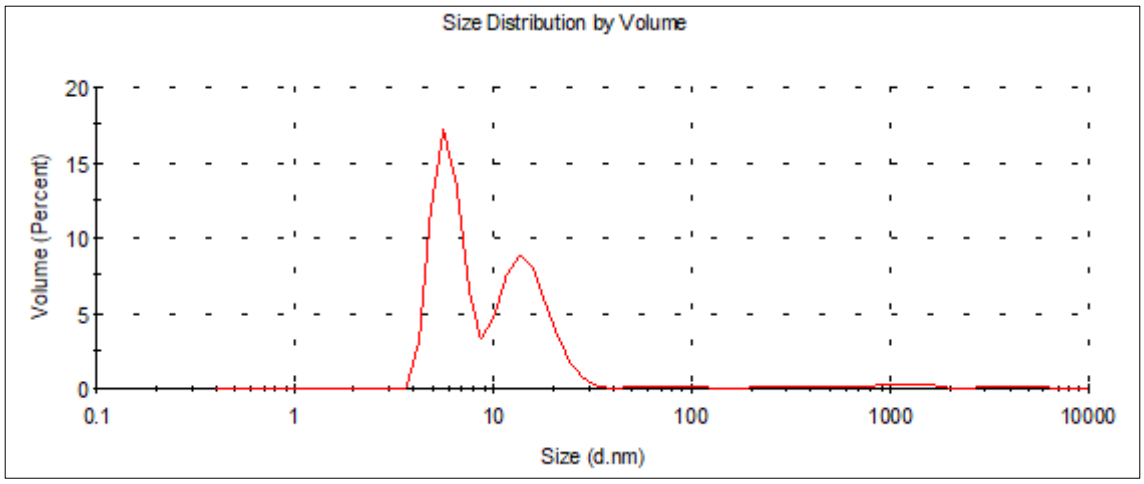

Fig 4: DLS measurement for Ag-Zn core-shell

Figure 4 depicts the size distribution of the nanoparticles that were prepared. Using dynamic light scattering (DLS) analysis, the size distribution and polydispersity index (PDI) of the Ag-Zn nanoparticles were determined. The analysis revealed the existence of smaller particles measuring 8 nm, constituting 69% of the distribution, and particles measuring 16 nm, making up the remaining 31%. Additionally, the Z-average size and PDI values for the synthesized nanoparticles were measured as 15.1 nm and 0.39, respectively, as reported in reference [35]. This data provides further insight into the average size and the extent of size variation among the nanoparticles. Such measurements are crucial for understanding the uniformity and dispersion of nanoparticles in a sample, which in turn can impact their behavior and performance in various applications.

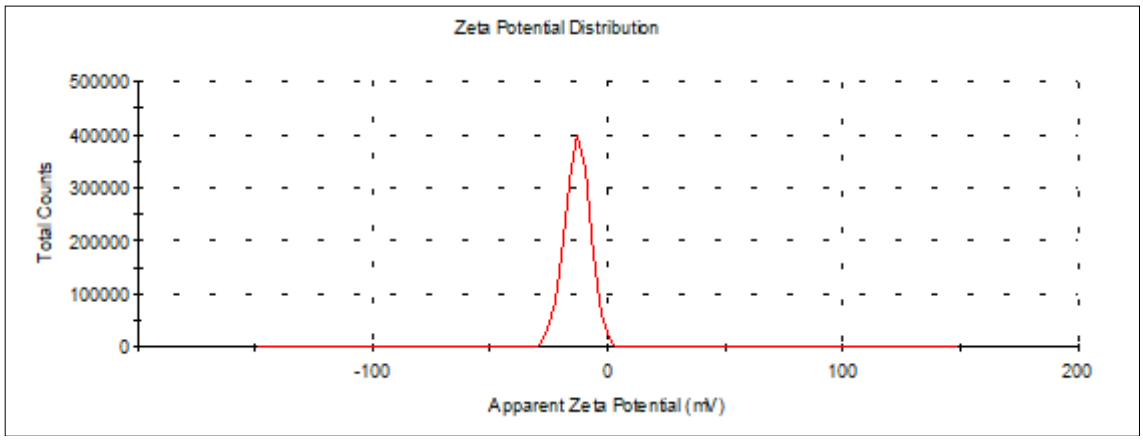

Fig 5: Zeta potential of Ag-Zn NPs

Figure 5 displays the zeta potential distribution concerning the Ag-Zn nanoparticles. Zeta potential is a crucial parameter that indicates the surface charge and stability of nanoparticles in a solution. In this case, the zeta potential value for the synthesized nanoparticles was determined to be -31 mV. This negative zeta potential suggests that the nanoparticles possess a sufficient surface charge to prevent aggregation or coagulation, thereby enhancing their stability in the dispersion. A more negative zeta potential indicates a higher repulsive force between nanoparticles, leading to improved suspension stability. The observed zeta potential value of -31 mV underlines the adequate charge on the nanoparticle surfaces, promoting their even distribution and minimizing the potential for undesirable agglomeration. This characterization of zeta potential contributes to a comprehensive understanding of the colloidal behavior and potential applications of the synthesized Ag-Zn nanoparticles.

UV-Visible spectroscopy

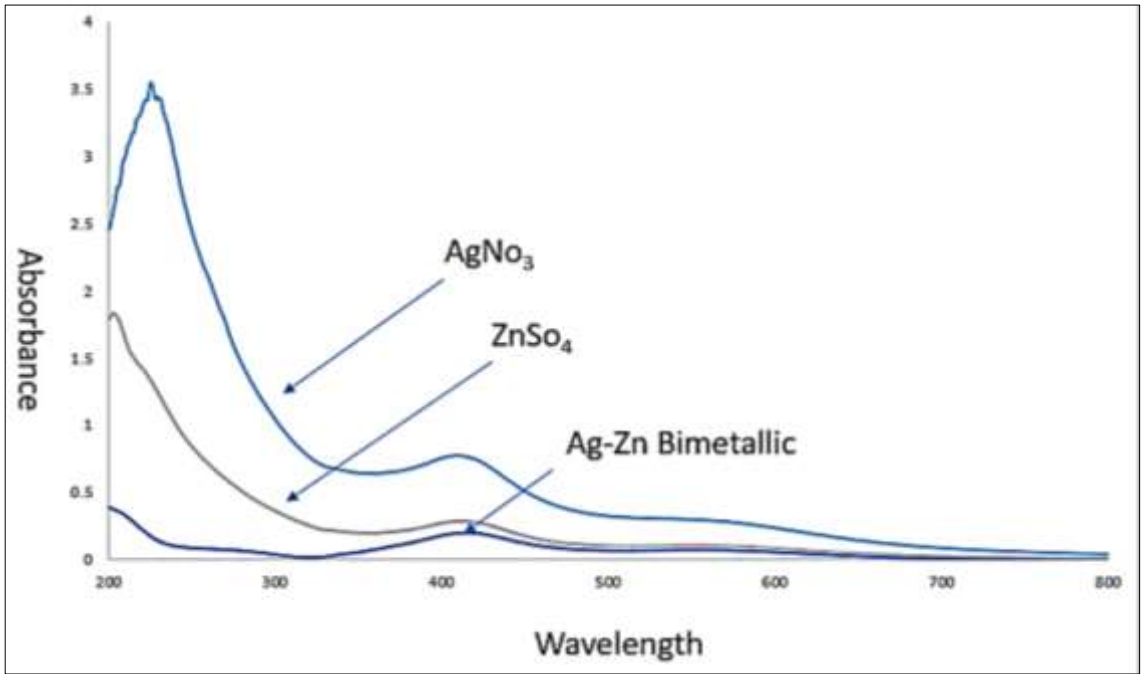

Fig 6: UV-Visible spectrum of bimetallic Ag-Zn NPs

The UV-Vis absorbance spectra were recorded using a UV-2450 instrument from Shimadzu, as depicted in Figure 6. Notably, a pronounced absorption peak was identified around 420 nm for the silver component. This absorption peak is attributed to the phenomenon of surface plasmon resonance (SPR) absorption, which is characteristic of silver nanoparticles. In contrast, the UV spectrum of pure zinc exhibited its own SPR band, notably peaking at 360 nm.

Interestingly, the UV spectrum of the Ag-Zn bimetallic nanoparticles demonstrated an absorption peak ranging from 390 to 400 nm. This absorption profile falls between the distinct peaks of pure silver and zinc nanoparticles. This observation strongly suggests the coexistence of both silver and zinc within a single particle, providing compelling evidence for the formation of an alloy structure. These results from the UV-Vis spectra provide valuable insights into the composition and structural characteristics of the synthesized Ag-Zn nanoparticles. The absorption peaks observed at intermediate wavelengths confirm the successful synthesis of bimetallic nanoparticles and underscore the presence of an alloyed structure, where both silver and zinc components contribute to the optical properties of the material.

Fourier Transform IR Spectroscopy

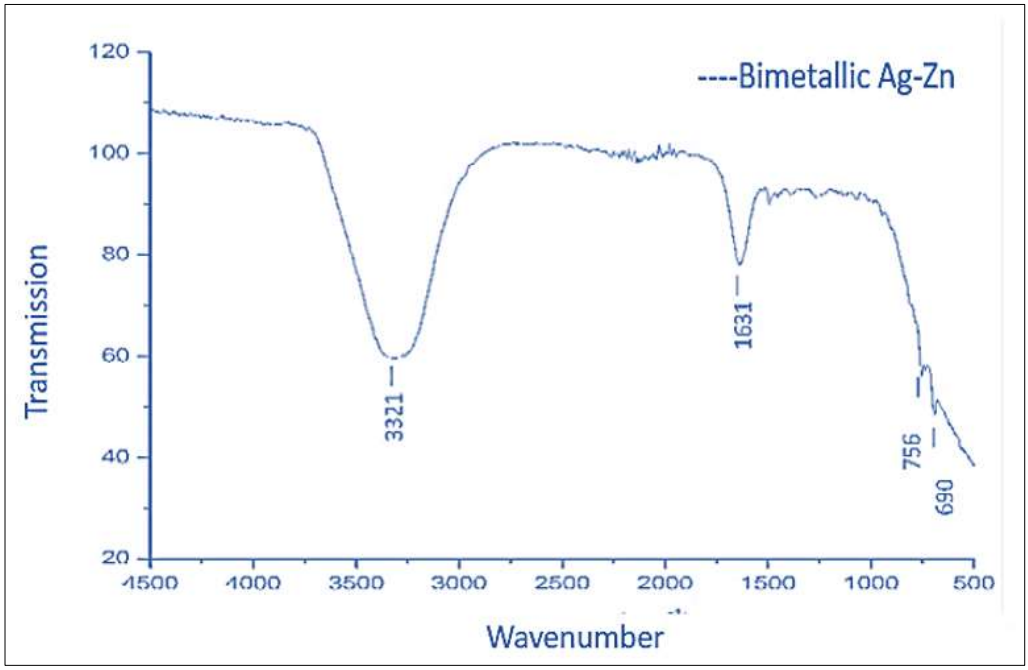

Fig 7: IR spectrum of bimetallic Ag-Zn nanoparticles

In Figure 7, the FT-IR spectrum of the synthesized Ag-Zn nanoparticles is depicted, revealing the presence of distinct functional groups within the Ag-Zn particles. The observed IR spectrum of Ag-Zn nanoparticles showcased broad and robust peaks at 3321 and 1631 cm^{-1}, respectively. These peaks serve as conclusive evidence for the binding of polyphenols and amino acids [36]. This finding aligns with the notion that polyphenols and amino acids have played a crucial role in reducing silver and zinc ions, facilitating the formation of silver-zinc bimetallic quantum dots. The presence of these specific functional groups indicates the involvement of bioactive molecules from the synthesis process, contributing to the stabilization and formation of the bimetallic nanoparticles. This FT-IR analysis provides valuable insights into the chemical interactions and mechanisms that underpin the successful synthesis of Ag-Zn nanoparticles, shedding light on the role of biomolecules in nanoparticle formation and stabilization.

Scanning Electron Microscopy

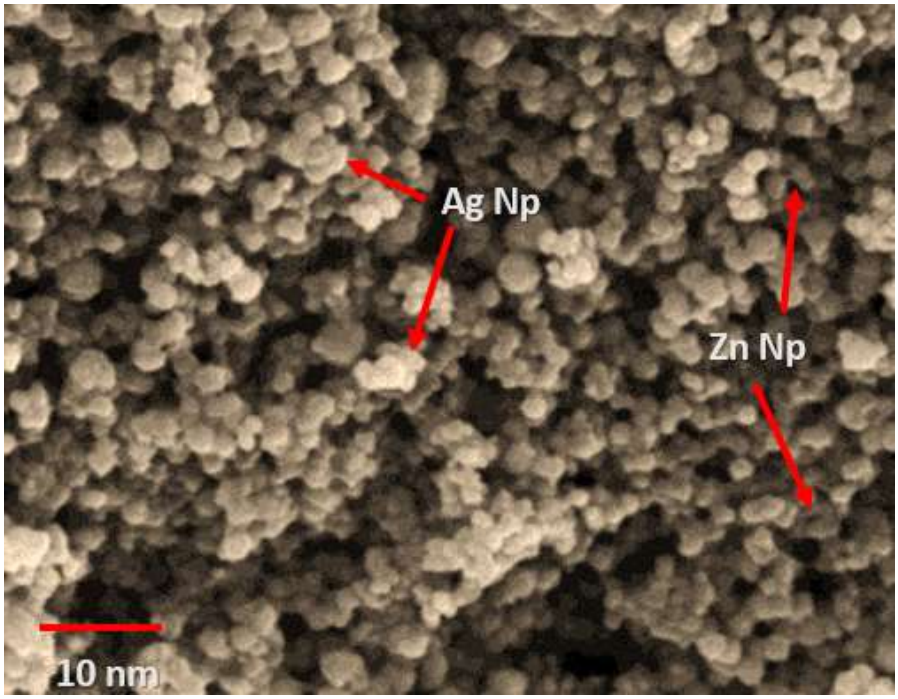

Fig 8: SEM image of synthesized bimetallic Ag-Zn NPs

The SEM images of the Ag-Zn bimetallic nanoparticles depict predominantly spherical or quasi-spherical particles spanning a size range of 8 to 13 nm. These images also potentially unveil agglomerated nanoparticles, a phenomenon attributable to their elevated surface energy. It's important to note that the morphology and size of the nanoparticles could exhibit variations contingent on the specific synthesis method employed and the experimental parameters [37-38]. This observed diversity underscores the sensitivity of nanoparticle characteristics to the intricate interplay of synthesis conditions, highlighting the need for precise control over these factors to achieve desired properties. The SEM imaging provides crucial visual insights into the structural attributes of the Ag-Zn nanoparticles, shedding light on their size distribution, shape, and potential aggregation tendencies.

Investigation of Antimicrobial Activity

The antibacterial activity of various substances, namely Madagascar periwinkle extract, silver nitrate, and zinc sulphate, as well as bimetallic Ag-Zn NPs was evaluated against both Gram-positive and Gram-negative bacteria. The findings demonstrated that bimetallic Ag-Zn NPs, at a concentration of 1000 µg/ml, exhibited significant antibacterial effects against *Pseudomonas aeruginosa*, *Escherichia coli*, *Bacillus subtilis*, *Staphylococcus aureus*, and *Enterococcus faecalis*, resulting in inhibition zones measuring 24.2 mm, 16.6 mm, 30.1 mm, 20.7 mm, and 13.9 mm, respectively.

Additionally, *Bacillus subtilis* displayed the highest sensitivity to bimetallic Ag-Zn NPs, with a minimum inhibitory concentration (MIC) of 15.32 µg/ml, while *Enterococcus faecalis* exhibited the lowest sensitivity, with an MIC of 250 µg/ml. Furthermore, the MIC values of bimetallic Ag-Zn NPs against *Escherichia coli*, *Pseudomonas aeruginosa*, and *Staphylococcus aureus* were determined as 62.5 µg/ml, 125 µg/ml, and 62.5 µg/ml, respectively.

On the other hand, Madagascar periwinkle extract displayed limited antibacterial activity, specifically against *Escherichia coli* and *Bacillus subtilis*. Neither silver nitrate nor zinc sulphate exhibited any antibacterial effects against the tested bacterial strains. These results indicate that the effectiveness of bimetallic Ag-Zn NPs cannot be solely attributed to their starting materials but rather to the properties and characteristics of the prepared nanoparticles themselves.

The mechanism of action underlying the antibacterial activity of bimetallic Ag-Zn NPs appears to involve several factors. Electrostatic interactions may cause damage to the bacterial cell membrane, disrupt proteins and enzymes, generate reactive oxygen species (ROS), and induce oxidative stress. The NPs may also bind to proteins, disrupting cellular homeostasis, including the electron transport chain and signal transduction pathways, potentially

leading to genotoxic effects. Moreover, the rough external surface of Ag-Zn NPs may contribute to cell wall damage, allowing the nanoparticles to penetrate the bacterial plasma membrane and exert toxic effects on the bacteria.

Table 1: Data for antibacterial activity of different samples

Bacterial Strain	Madagascar Periwinkle Extract	Silver Nitrate	Zinc Sulphate	Bimetallic Ag-Zn NPs
Pseudomonas aeruginosa	0	0	0	24.2
Escherichia coli	X	0	0	16.6
Bacillus subtilis	X	0	0	30.1
Staphylococcus aureus	0	0	0	20.7
Enterococcus faecalis	0	0	0	13.9

(Please note that in the table above, "X" indicates limited antibacterial activity, and "0" indicates no antibacterial activity.)

Table 2: MIC values of bacterial strains

Bacterial Strain	MIC (µg/ml)
Escherichia coli	62.5
Pseudomonas aeruginosa	125
Staphylococcus aureus	62.5
Bacillus subtilis	15.32
Enterococcus faecalis	250

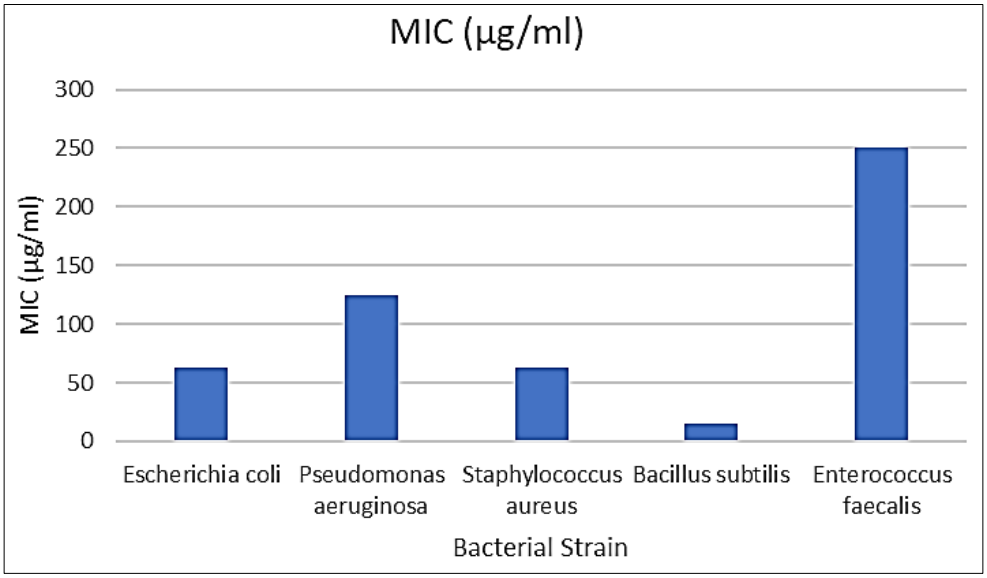

Fig 9: MIC values of bacterial strains

Investigation of Antifungal Activity

The antifungal activity of the initial substances and bimetallic Ag-Zn NPs was examined against *Candida albicans*, *Cryptococcus neoformans*, *Aspergillus brasiliensis*, and *Aspergillus fumigatus*. The results demonstrated that the bimetallic Ag-Zn NPs possessed potent antifungal properties against both unicellular and multicellular fungi.

The synthesized bimetallic Ag-Zn NPs exhibited inhibitory effects on *C. albicans*, C. *neoformans*, *A. brasiliensis*, and *A. fumigatus*, generating inhibition zones measuring 37.2, 36.7, 31.2, and 20.7 mm, respectively, at a concentration of 1000 µg/ml.

Furthermore, the minimum inhibitory concentration (MIC) of the bimetallic Ag-Zn NPs against each fungal strain was determined. The MIC values indicated that the bimetallic Ag-Zn NPs exhibited MICs of 7.81, 31.25, 62.5, and 125 µg/ml against *C. albicans*, *C. neoformans*, *A. brasiliensis*, and *A. fumigatus*, respectively. These findings confirm the high efficacy of the bimetallic Ag-Zn NPs against unicellular fungi compared to multicellular fungi. Notably, *C. albicans* displayed the greatest sensitivity among the tested strains [39-41].

In contrast, silver nitrate and zinc sulphate displayed no antifungal activity, while higher concentrations (500-1000 µg/ml) demonstrated weak antifungal activity

Table 3: Fungal strains and inhibition zones

Fungal strains	Inhibition Zones (mm)	Minimum Inhibitory Concentration (MIC) values (µg/ml)
Candida albicans	37.2	7.81
Cryptococcus neoformans	36.7	31.25
Aspergillus brasiliensis	31.2	62.5
Aspergillus fumigatus	20.7	125

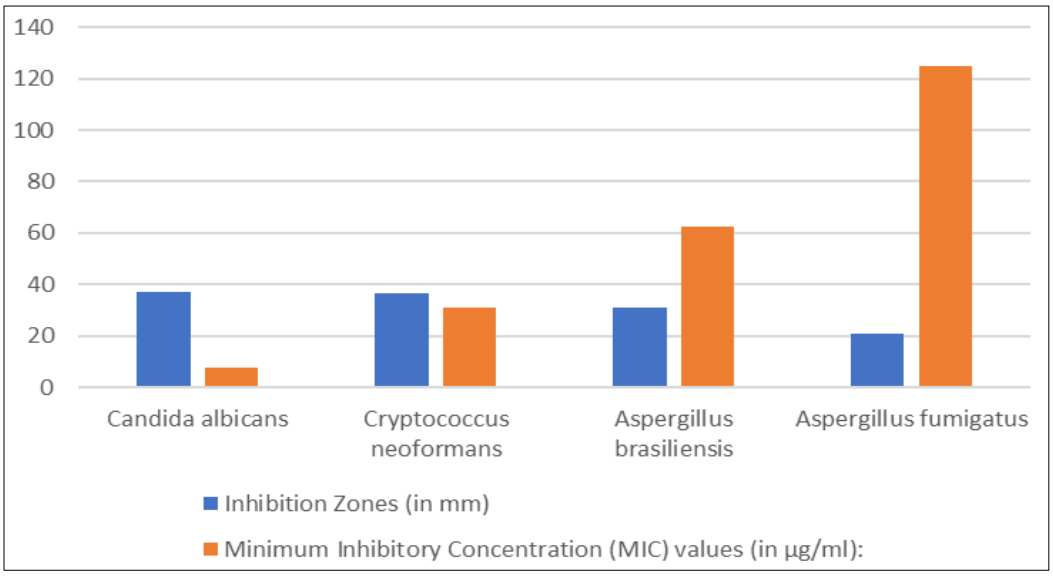

Fig 10: Inhibition zones and minimum inhibitory concentrations

Investigation of Anticancer Activity

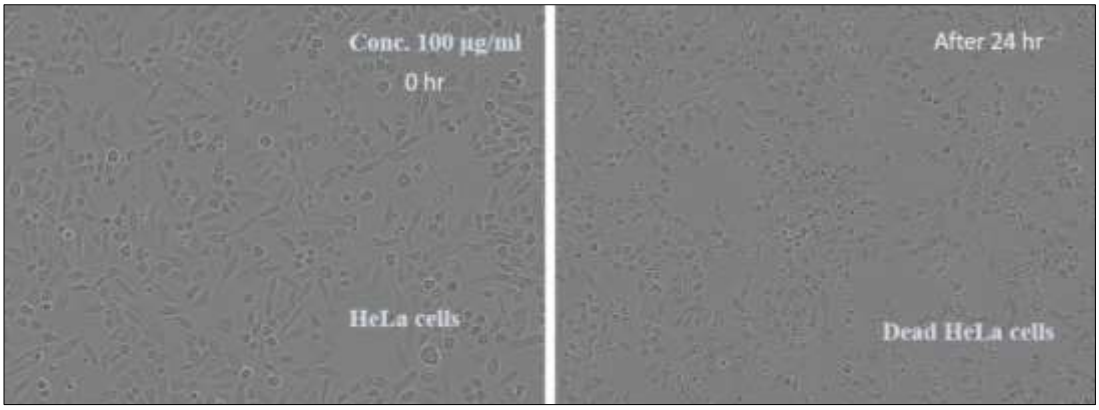

Fig 11: 20x magnified HeLa cells 0 hr and 24 hr after Ag-Zn treatment

Potential anticancer properties of biologically synthesized bimetallic silver-zinc NPs against HeLa cancer cells were evaluated. The results obtained from this study unveiled significant anticancer effects of the bimetallic Ag-Zn NPs on the cancerous cell lines, with an IC50 value of 52.4 µg/ml.

Furthermore, a detailed assessment of the anticancer activity of the bimetallic Ag-Zn NPs was conducted by exposing HeLa cells to varying concentrations of 5, 25, 65, and 100 µg/ml. The findings demonstrated that the bimetallic Ag-Zn NPs exhibited high effectiveness in inhibiting the growth of HeLa cells, with observed percentages of inhibition reaching 97.7%, 97.6%, 93.2%, and 67.1%, respectively, corresponding to the aforementioned concentrations.

These outcomes suggest that the biosynthesized bimetallic Ag-Zn NPs possess promising potential as an anticancer agent, particularly in combating the growth and proliferation of HeLa cancer cells.

Table 4: Study of anticancer activity of Ag-Zn NPs

Compound name	Conc. (µg/ml)	OD at 590 nm	% Viability of HeLa cells
Control	0	1.590 ± 0.081	100
Ag-Zn	5	0.494 ± 0.046	31
	25	0.404 ± 0.100	25
	65	0.225 ± 0. 055	14
	100	0.133 ± 0.112	3

Conclusion

In conclusion, the one-pot synthesis of bimetallic Ag-Zn NPs using Madagascar periwinkle (*Catharanthus roseus*) extract as a reducing and stabilizing agent has been successfully demonstrated. The use of natural plant extracts as a green and sustainable alternative to traditional chemical methods for NP synthesis has gained significant attention in recent years due to their low toxicity and abundance of reducing agents.

The synthesized bimetallic Ag-Zn NPs were characterized using various analytical techniques, including UV-Vis spectroscopy, DLS, and Fourier Transform Infrared spectroscopy (FTIR). The results showed that the NPs were spherical in shape and had an average size of 8-12 nm. The nanoparticles also exhibited excellent stability and biocompatibility, making them suitable for various biomedical applications.

Furthermore, the synthesized nanoparticles displayed potent antimicrobial activity against both Gram-positive and Gram-negative bacteria, indicating their potential use as antibacterial agents. The nanoparticles also exhibited cytotoxicity against cancer cell lines, demonstrating their potential use as anticancer agents. These results suggest that the nanodrugs Ag-Zn, have good potency in Cervical cancer (HeLa cells) with only 3% viable cells present in maximum concentration (100 µg/ml).

Overall, the one-pot synthesis of bimetallic Ag-Zn NPs using Madagascar periwinkle extract offers a promising

green and sustainable approach for the synthesis of biologically active NPs with potential applications in various fields, including biomedicine and environmental remediation.

Data availability

The corresponding authors can provide the supporting data for this study upon a reasonable request.

Conflicts of interest

The authors do not possess any conflicts of interest to disclose.

References

1. Nadeem M, Tungmunnithum D, Hano C, Abbasi BH, Hashmi SS, Ahmad W, *et al*. The current trends in the green syntheses of titanium oxide nanoparticles and their applications. Green chemistry letters and reviews. 2018 Oct 2;11(4):492-502. doi: 10.1080/17518253.2018.1538430. [CrossRef] [Google Scholar]
2. Saleem K, Khursheed Z, Hano C, Anjum I, Anjum S. Applications of nanomaterials in leishmaniasis: a focus on recent advances and challenges. Nanomaterials. 2019 Dec 9;9(12):1749. doi:10.3390/nano9121749. [PMC free article] [PubMed] [CrossRef] [Google Scholar]
3. Anjum S, Anjum I, Hano C, Kousar S. Advances in nanomaterials as novel elicitors of pharmacologically active plant specialized metabolites: Current status and future outlooks. RSC advances. 2019;9(69):40404-23. doi: 10.1039/C9RA08457F. [CrossRef] [Google Scholar]
4. Gul R, Jan H, Lalay G, Andleeb A, Usman H, Zainab R, *et al*. Medicinal plants and biogenic metal oxide nanoparticles: a paradigm shift to treat Alzheimer's disease. Coatings. 2021 Jun 15;11(6):717. doi: 10.3390/coatings11060717. [CrossRef] [Google Scholar]
5. Shafiq M, Anjum S, Hano C, Anjum I, Abbasi BH. An overview of the applications of nanomaterials and nanodevices in the food industry. Foods. 2020 Feb 3;9(2):148. Doi:10.3390/foods9020148. [PMC free article] [PubMed] [CrossRef] [Google Scholar]
6. Chaudhary R, Nawaz K, Khan AK, Hano C, Abbasi BH, Anjum S. An overview of the algae-mediated biosynthesis of nanoparticles and their biomedical applications. Biomolecules. 2020 Oct 30;10(11):1498. Doi: 10.3390/biom10111498. [PMC free article] [PubMed] [CrossRef] [Google Scholar]
7. Abbasi BH, Fazal H, Ahmad N, Ali M, Giglioli-Guivarch N, Hano C, *et al*. Nanomaterials for cosmeceuticals: Nanomaterials-induced advancement in cosmetics, challenges, and opportunities. Nanocosmetics. 2020 Jan 1:79-108.
8. Letchumanan D, Sok SP, Ibrahim S, Nagoor NH, Arshad NM. Plant-based biosynthesis of copper/copper oxide nanoparticles: an update on their applications in biomedicine, mechanisms, and toxicity. Biomolecules. 2021 Apr 12;11(4):564. Doi: 10.3390/biom11040564. [PMC free article] [PubMed] [CrossRef] [Google Scholar]
9. Jadoun S, Arif R, Jangid NK, Meena RK. Green synthesis of nanoparticles using plant extracts: A review. Environmental Chemistry Letters. 2021 Feb;19:355-74. doi:10.1007/s10311-020-01074-x. [CrossRef] [Google Scholar]
10. Anjum S, Ishaque S, Fatima H, Farooq W, Hano C, Abbasi BH, *et al*. Emerging applications of nanotechnology in healthcare systems: Grand challenges and perspectives. Pharmaceuticals. 2021 Jul 21;14(8):707. Doi:10.3390/ph14080707. [PMC free article] [PubMed] [CrossRef] [Google Scholar]
11. Khan AK, Renouard S, Drouet S, Blondeau JP, Anjum I, Hano C, *et al*. Effect of uv irradiation (a and c) on casuarina equisetifolia-mediated biosynthesis and characterization of antimicrobial and anticancer activity of biocompatible zinc oxide nanoparticles. Pharmaceutics. 2021 Nov 22;13(11):1977. doi: 10.3390/pharmaceutics13111977. [PMC free article] [PubMed] [CrossRef] [Google Scholar]
12. Anjum S, Hashim M, Malik SA, Khan M, Lorenzo JM, Abbasi BH, *et al.* Recent advances in zinc oxide nanoparticles (ZnO NPs) for cancer diagnosis, target drug delivery, and treatment. Cancers. 2021 Sep 12;13(18):4570. doi: 10.3390/cancers13184570. [PMC free article] [PubMed] [CrossRef] [Google Scholar]
13. Andleeb A, Andleeb A, Asghar S, Zaman G, Tariq M, Mehmood A, *et al*. A systematic review of biosynthesized metallic nanoparticles as a promising anti-cancer-strategy. Cancers. 2021 Jun 5;13(11):2818. doi: 10.3390/cancers13112818. [PMC free article] [PubMed] [CrossRef] [Google Scholar]
14. Khan T, Abbasi BH, Afridi MS, Tanveer F, Ullah I, Bashir S, *et al*. Melatonin-enhanced biosynthesis of antimicrobial AgNPs by improving the phytochemical reducing potential of a callus culture of Ocimum basilicum L. var. thyrsiflora. RSC advances. 2017;7(61):38699-713. [Google Scholar]
15. Jan H, Shah M, Usman H, Khan MA, Zia M, Hano C, *et al*. Biogenic synthesis and characterization of antimicrobial and antiparasitic zinc oxide (ZnO) nanoparticles using aqueous extracts of the Himalayan Columbine (*Aquilegia pubiflora*). Frontiers in Materials. 2020 Aug 12;7:249. doi: 10.3389/fmats.2020.00249. [CrossRef] [Google Scholar]
16. Shah M, Nawaz S, Jan H, Uddin N, Ali A, Anjum S, *et al.* Synthesis of bio-mediated silver nanoparticles from Silybum marianum and their biological and clinical activities. Materials Science and Engineering: C. 2020 Jul 1;112:110889. doi: 10.1016/j.msec.2020.110889. [PubMed] [CrossRef] [Google Scholar]
17. Clark JH, Macquarrie DJ. Handbook of Green Chemistry and Technology. John Wiley & Sons; Hoboken, NJ, USA; c2008. [Google Scholar]
18. Robert KW, Parris TM, Leiserowitz AA. What is sustainable development? Goals, indicators, values, and practice. Environment: science and policy for sustainable development. 2005 Apr 1;47(3):8-21. doi: 10.1080/00139157.2005.10524444. [CrossRef] [Google Scholar]
19. Omer AM. Energy, environment and sustainable development. Renewable and sustainable energy reviews. 2008 Dec 1;12(9):2265-300. doi: 10.1016/j.rser.2007.05.001. [CrossRef] [Google Scholar]
20. Nath D, Banerjee P. Green nanotechnology–a new hope for medical biology. Environmental toxicology and pharmacology. 2013 Nov 1;36(3):997-1014. doi:

10.1016/j.etap.2013.09.002. [PubMed] [Cross Ref] [Google Scholar]
21. Razavi M, Salahinejad E, Fahmy M, Yazdimamaghani M, Vashaee D, Tayebi L, *et al*. Green chemical and biological synthesis of nanoparticles and their biomedical applications. Green Processes for Nanotechnology: From Inorganic to Bioinspired Nanomaterials. 2015:207-35. [Google Scholar]
22. Narayanan KB, Sakthivel N. Green synthesis of biogenic metal nanoparticles by terrestrial and aquatic phototrophic and heterotrophic eukaryotes and biocompatible agents. Advances in colloid and interface science. 2011 Dec 12;169(2):59-79. doi: 10.1016/j.cis.2011.08.004. [PubMed] [CrossRef] [Google Scholar]
23. Mallikarjuna K, Nasif O, Ali Alharbi S, Chinni SV, Reddy LV, Reddy MR, *et al.* Phytogenic synthesis of Pd-Ag/rGO nanostructures using stevia leaf extract for photocatalytic H2 production and antibacterial studies. Biomolecules. 2021 Jan 29;11(2):190. doi: 10.3390/biom11020190. [PMC free article] [PubMed] [CrossRef] [Google Scholar]
24. Khan SA, Shahid S, Lee CS. Green synthesis of gold and silver nanoparticles using leaf extract of *Clerodendrum inerme*; characterization, antimicrobial, and antioxidant activities. Biomolecules. 2020 May 29;10(6):835. doi: 10.3390/biom10060835. [PMC free article] [PubMed] [CrossRef] [Google Scholar]
25. Khan SA, Shahid S, Shahid B, Fatima U, Abbasi SA. Green synthesis of MnO nanoparticles using abutilon indicum leaf extract for biological, photocatalytic, and adsorption activities. Biomolecules. 2020 May 19;10(5):785. doi: 10.3390/biom10050785. [PMC free article] [PubMed] [CrossRef] [Google Scholar]
26. Alshehri AA, Malik MA. Phytomediated photo-induced green synthesis of silver nanoparticles using *Matricaria chamomilla* L. and its catalytic activity against rhodamine B. Biomolecules. 2020 Nov 26;10(12):1604. doi: 10.3390/biom10121604. [PMC free article] [PubMed] [CrossRef] [Google Scholar]
27. Singh R, Hano C, Nath G, Sharma B. Green biosynthesis of silver nanoparticles using leaf extract of *Carissa carandas* L. and their antioxidant and antimicrobial activity against human pathogenic bacteria. Biomolecules. 2021 Feb 17;11(2):299. doi: 10.3390/biom11020299. [PMC free article] [PubMed] [CrossRef] [Google Scholar]
28. Zaeem A, Drouet S, Anjum S, Khurshid R, Younas M, Blondeau JP, *et al.* Effects of biogenic zinc oxide nanoparticles on growth and oxidative stress response in flax seedlings vs. *in vitro* cultures: A comparative analysis. Biomolecules. 2020 Jun 17;10(6):918. doi: 10.3390/biom10060918. [PMC free article] [PubMed] [CrossRef] [Google Scholar]
29. Srihasam S, Thyagarajan K, Korivi M, Lebaka VR, Mallem SP. Phytogenic generation of NiO nanoparticles using Stevia leaf extract and evaluation of their in-vitro antioxidant and antimicrobial properties. Biomolecules. 2020 Jan 6;10(1):89. doi: 10.3390/biom10010089. [PMC free article] [PubMed] [CrossRef] [Google Scholar]
30. Wahid I, Kumari S, Ahmad R, Hussain SJ, Alamri S, Siddiqui MH, *et al.* Silver nanoparticle regulates salt tolerance in wheat through changes in ABA concentration, ion homeostasis, and defense systems. Biomolecules. 2020 Nov 2;10(11):1506. doi: 10.3390/biom10111506. [PMC free article] [PubMed] [CrossRef] [Google Scholar]
31. Hossain A, Abdallah Y, Ali MA, Masum MM, Li B, Sun G, *et al.* Lemon-fruit-based green synthesis of zinc oxide nanoparticles and titanium dioxide nanoparticles against soft rot bacterial pathogen *Dickeya dadantii*. Biomolecules. 2019 Dec 11;9(12):863. doi: 10.3390/biom9120863. [PMC free article] [PubMed] [CrossRef] [Google Scholar]
32. Ahmad H, Venugopal K, Rajagopal K, De Britto S, Nandini B, Pushpalatha HG, *et al.* Green Synthesis and Characterization of Zinc Oxide Nanoparticles Using *Eucalyptus globules* and Their Fungicidal Ability Against Pathogenic Fungi of Apple Orchards. Biomolecules. 2020;10(3):425. doi: 10.3390/biom10030425. [PMC free article] [PubMed] [CrossRef] [Google Scholar]
33. Cherian T, Ali K, Saquib Q, Faisal M, Wahab R, Musarrat J. Cymbopogon citratus functionalized green synthesis of CuO-nanoparticles: Novel prospects as antibacterial and antibiofilm agents. Biomolecules. 2020 Jan 22;10(2):169. doi: 10.3390/biom10020169. [PMC free article] [PubMed] [CrossRef] [Google Scholar]
34. Prasad KS, Prasad SK, Ansari MA, Alzohairy MA, Alomary MN, AlYahya S, *et al.* Tumoricidal and bactericidal properties of ZnONPs synthesized using *Cassia auriculata* leaf extract. Biomolecules. 2020 Jun 30;10(7):982. doi: 10.3390/biom10070982. [PMC free article] [PubMed] [CrossRef] [Google Scholar]
35. Silva Viana RL, Pereira Fidelis G, Jane Campos Medeiros M, Antonio Morgano M, Gabriela Chagas Faustino Alves M, *et al.* Green synthesis of antileishmanial and antifungal silver nanoparticles using corn cob xylan as a reducing and stabilizing agent. Biomolecules. 2020 Aug 25;10(9):1235. doi: 10.3390/biom10091235. [PMC free article] [PubMed] [CrossRef] [Google Scholar]
36. Ansari MA, Murali M, Prasad D, Alzohairy MA, Almatroudi A, Alomary MN, *et al.* Cinnamomum verum bark extract mediated green synthesis of ZnO nanoparticles and their antibacterial potentiality. Biomolecules. 2020 Feb 19;10(2):336. doi: 10.3390/biom10020336. [PMC free article] [PubMed] [CrossRef] [Google Scholar]
37. Perveen K, Husain FM, Qais FA, Khan A, Razak S, Afsar T, *et al.* Microwave-assisted rapid green synthesis of gold nanoparticles using seed extract of *Trachyspermum ammi*: ROS mediated biofilm inhibition and anticancer activity. Biomolecules. 2021 Jan 30;11(2):197. doi: 10.3390/biom11020197. [PMC free article] [PubMed] [CrossRef] [Google Scholar]
38. Mickymaray S. One-step synthesis of silver nanoparticles using Saudi Arabian desert seasonal plant *Sisymbrium irio* and antibacterial activity against multidrug-resistant bacterial strains. Biomolecules. 2019 Oct 28;9(11):662. doi: 10.3390/biom9110662. [PMC free article] [PubMed] [CrossRef] [Google Scholar]
39. Tolaymat TM, El Badawy AM, Genaidy A, Scheckel KG, Luxton TP, Suidan M, *et al*. An evidence-based environmental perspective of manufactured silver nanoparticle in syntheses and applications: A systematic review and critical appraisal of peer-reviewed scientific papers. Science of the total environment. 2010 Feb 1;408(5):999-1006. doi:

10.1016/j.scitotenv.2009.11.003. [PubMed] [CrossRef] [Google Scholar]
40. Ghosh P, Han G, De M, Kim CK, Rotello VM. Gold nanoparticles in delivery applications. Advanced drug delivery reviews. 2008 Aug 17;60(11):1307-15. [PubMed] [Google Scholar]
41. Jain PK, Lee KS, El-Sayed IH, El-Sayed MA. Calculated absorption and scattering properties of gold nanoparticles of different size, shape, and composition: applications in biological imaging and biomedicine. The journal of physical chemistry B. 2006 Apr 13;110(14):7238-48. doi: 10.1021/jp057170o. [PubMed] [CrossRef] [Google Scholar]